Spectroscopic and theoretical evidence for the photoinduced twisted intramolecular charge transfer state formation in N, N-dimethylaminonaphthyl-(acrylo)-nitrile

ARTICLE *in* JOURNAL OF LUMINESCENCE · SEPTEMBER 2008

Impact Factor: 2.72 · DOI: 10.1016/j.jlumin.2008.01.015

4 AUTHORS, INCLUDING:

Rupashree Balia Singh
National Institute of Advanced Industrial Sc…
27 PUBLICATIONS **419** CITATIONS
SEE PROFILE

Subrata Mahanta
National Institute of Advanced Industrial Sc…
25 PUBLICATIONS **398** CITATIONS
SEE PROFILE

Available online at www.sciencedirect.com
ScienceDirect
Journal of Luminescence 128 (2008) 1421–1430
JOURNAL OF LUMINESCENCE
www.elsevier.com/locate/jlumin

Spectroscopic and theoretical evidence for the photoinduced twisted intramolecular charge transfer state formation in *N*,*N*-dimethylaminonaphthyl-(acrylo)-nitrile

Rupashree Balia Singh, Subrata Mahanta, Samiran Kar[1], Nikhil Guchhait*

Department of Chemistry, University of Calcutta, 92, A. P. C. Road, Kolkata 700009, India

Received 2 November 2007; received in revised form 18 January 2008; accepted 23 January 2008
Available online 7 February 2008

Abstract

The phenomenon of excited state twisted intramolecular charge transfer (TICT) process in *N*,*N*-dimethylaminonaphthyl-(acrylo)-nitrile (DMANAN) has been reported on the basis of steady-state absorption and fluorescence spectroscopy in combination with quantum chemical calculations. The absorption and fluorescence characteristics of DMANAN in solvents of different polarity reveal the presence of a single species in the ground state which forms the intramolecular charge transfer state upon photoexcitation. The observed dual fluorescence is assigned to a high-energy emission from the locally excited or the Franck–Condon state and the red-shifted emission from the charge transfer (CT) state. In polar protic solvents, hydrogen-bonding interaction on CT emission has been established from the linear dependency of the position of the low-energy emission maxima on hydrogen-bonding parameter (α). The experimental findings have been correlated with the theoretical results based on TICT model obtained at density functional theory (DFT) level. The theoretical potential energy surface for the first excited state along both the donor and acceptor twist coordinates in the gas phase obtained by time dependent density functional theory (TDDFT) method and in polar solvent by time dependent density functional theory-polarized continuum model (TDDFT-PCM) method predicts well the experimental spectral properties.

Keywords: *N*, *N*-dimethylaminonaphthyl-(acrylo)-nitrile; TICT; Absorption; Fluorescence; Density functional theory

1. Introduction

The basic process involved in the excited state intramolecular charge transfer (ICT) reactions is an interesting arena for researchers in the field of physical chemistry and chemical physics. Even after decades of the discovery of dual fluorescence in 4-*N*,*N*-dimethylaminobenzonitrile (DMABN) by Lippert et al. [1], new molecules are being designed for the possibility of photoinduced ICT reaction [2–15]. The need for new donor–acceptor charge transfer (CT) molecules crops up due to their vast applications in the field of pure and applied sciences such as pH and ion detectors, sensors for free volume in polymers, study of micro-heterogeneous environments, etc. to mention a few [16,17]. The need and interest for new molecules multiplied when it became clear that photoinduced ICT may play a crucial role in biological light-harvesting processes such as photosynthesis [18]. The dual fluorescence of the benchmark molecule DMABN has been studied from experimental and theoretical perspectives for describing ICT process over the past few decades [19–23]. In DMABN, the higher energy band from L_b state arises due to normal fluorescence, whereas the lower energy (LE) band from L_a state is described as the "anomalous" fluorescence band from the CT state. The past years have however witnessed the rise of different schools, which did not agree in their views of the ICT state. Broadly classifying, three different theoretical models have been described to explain the observed anomalous emission of the molecules exhibiting ICT process. These are mainly (i) twisted intramolecular

*Corresponding author. Tel.: +91 33 2350 8386; fax: +91 33 2351 9755.
E-mail addresses: nikhil.guchhait@rediffmail.com, nguchhait@yahoo.com (N. Guchhait).
[1]Present address: CHEMGEN Pharma International, Dr. Siemens Street, Block GP, Sect. V, Salt Lake City, Kolkata 700091, India.

0022-2313/$ - see front matter © 2008 Published by Elsevier B.V.
doi:10.1016/j.jlumin.2008.01.015

charge transfer (TICT) [24–26], (ii) planarized intramolecular charge transfer (PICT) [27] and (iii) rehybridized intramolecular charge transfer [28]. Out of these models, the concept of TICT has been put to maximum use while explaining the ICT process in most cases. However, the PICT model put forward by Zachariasse and co-workers in a number of papers has also gained importance since 1993 [29,30]. In the concept of TICT, it is stated that in the twisted conformation the donor-NMe_2 group of DMABN is twisted 90° out of plane and hence completely decoupled from the acceptor nitrile group [24–26]. Under this condition, complete CT takes place and the L_a band is thought to be responsible for CT emission from this twisted conformer.

In the present work, we have investigated the ground and excited state properties of *N*,*N*-dimethylaminonaphthyl-(acrylo)-nitrile (DMANAN) spectroscopically. Till date, most of the systems studied for excited state TICT reaction consisted of donor and acceptor groups connected to benzene chromophore [5,12–15]. There are examples where substances other than benzene chromophore have been used to study ICT reaction for donor–acceptor systems. We have tried to explore the possibility of ICT process in naphthalene ring-containing systems for which there are very few examples [31,32]. Very recently, we have investigated donor–acceptor excited state CT reaction in naphthalene systems such as methyl ester of *N*,*N*-dimethylaminonaphthyl-(acrylic)-acid (MDMANA) and ethyl ester of *N*,*N*-dimethylaminonaphthyl-(acrylic)-acid (EDMANA) [33,34]. The title molecule has been synthesized, and the absorption and fluorescence spectroscopy have been used to study its photophysical behaviour. Theoretical calculations for the ground state structure have been performed at density functional theory (DFT) level using B3LYP functional and 6–31G** basis set. Exploration of the ground and excited state potential energy curves (PECs) along the donor and acceptor coordinates in vacuo at DFT level further reinforced the idea of TICT process in DMANAN. The PECs with inclusion of solvent effect have been evaluated using time dependent density functional theory-polarized continuum model (TDDFT-PCM) method to correlate the observed spectral properties and solvent polarity dependent red-shifted emission band.

2. Materials and methods

2.1. Materials

The molecule DMANAN was prepared from *p*-(dimethylamino) naphthaldehyde by standard procedure . In brief, *p*-(dimethylamino) naphthaldehyde and triphenylphosphoranylideneacetonitrile in dry dichloromethane were stirred at room temperature for several hours. After the solvent was removed over vacuum, the crude compound was purified by silica gel column chromatography and repeated crystallization with a minimum amount of methanol done to get pure product DMANAN (Scheme 1),

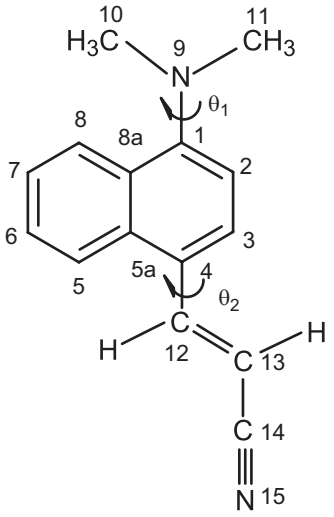

Scheme 1. Structure of DMANAN with numbering of atoms, θ_1 and θ_2 are donor and acceptor twist angles, respectively.

^{1}HNMR (400 MHz, $CHCl_3$): δ 3.02 (s, 6 H, –NMe_2), 5.87 (d, $J = 16.32$ Hz, 1H), 7.10 (m, 1H), 7.56–7.64 (m, 3H), 8.03 (m, 1H), 8.16 (d, $J = 16.33$ Hz, 1H), and 8.34 (m, 1H).

Spectroscopic grade hexane (HEX), cyclohexane (CYC), *n*-heptane (HEP), methylcyclohexane (MCH), tetrahydrofuran (THF), chloroform ($CHCl_3$), carbon tetrachloride (CCl_4), dioxane (DOX), methanol (MeOH), ethanol (EtOH), isopropanol (Iso-pr) and acetonitrile (ACN) solvents were purchased from Spectrochem and were used after proper distillation. Sulphuric acid from E Merck was used after proper vacuum distillation. Triple distilled water was used for the preparation of aqueous solutions. In all measurements, the sample concentration has been maintained within the range 10^{-4}–10^{-5} mol dm^{-3} in order to avoid aggregation and reabsorption effects.

The fluorescence quantum yields of the CT species of DMANAN in solvents of different polarity are measured relative to recrystallized β-naphthol ($\Phi_f = 0.23$ in MCH) as the secondary standard (Table 1) and calculated on the basis of the following equation:

$$\Phi_f = \Phi_f^{\circ} \frac{n_o^2 A^{\circ} \int I_f(\lambda_f)\, d\lambda_f}{n^2 A \int I_f^{\circ}(\lambda_f)\, d\lambda_f}$$

where n_o and n are the refractive indices of the solvents, A^o and A are the absorbances, Φ_f^o and Φ_f are the quantum yields, and the integrals denote the area of the fluorescence bands for the standard and the sample, respectively.

2.2. Steady-state measurements

The absorption and emission measurements were done by Hitachi UV–vis U-3501 spectrophotometer and Perkin Elmer LS-50B fluorimeter, respectively. In all measurements, the sample concentration was maintained within the range 10^{-4}–10^{-5} mol dm^{-3}. All measurements were done at room temperature if not otherwise mentioned.

Table 1
Spectroscopic parameters of *N,N*-dimethylaminonaphthyl-(acrylo)-nitrile (DMANAN) obtained from band maxima of absorption and emission spectra

Solvent	Absorption maxima (nm)	Fluorescence(nm)		φ_{LE}[a]	φ_{CT}[a]	ν_a (cm^{-1})	ν_f (cm^{-1})	($\nu_a-\nu_f$) (cm^{-1})
		λ_{LE}	λ_{CT}					
HEX	360	440	–	8.87	–	27,778	22,727	5051
HEP	361	443	–	11.92	–	27,701	22,573	5128
MCH	360	443	–	10.81	–	27,778	22,573	5205
CCl_4	373	430	473	–	7.81	26,809	21,142	5667
$CHCl_3$	375	430	473	–	9.21	26,667	21,142	5525
THF	370	430	472	–	11.23	27,027	21,186	5841
Iso-pr	371	430	473	–	13.11	26,954	21,142	5812
EtOH	370	430	480	–	15.45	27,027	20,833	6194
MeOH	370	430	486	–	18.43	27,027	20,576	6451
$MeOH+H^+$	310	423	474	–	–	32,258	23,641	8617
ACN	370	430	485	–	17.4	27,027	20,619	6408
Water	355	435	498	–	5.12	28,169	20,080	8089
DOX	366	430	468	–	18.88	27,322	21,368	5954

[a]Quantum yields are $\times 10^{-3}$

2.3. Computational procedures

The global minimum structure of DMANAN is obtained by optimizing the geometry at DFT level with B3LYP functional and 6–31G** basis set using Gaussian 03W version of the software [35]. There are several theoretical ways to map the potential energy surfaces of donor–acceptor charge transfer reactions. In our case the PECs for the ground and first two excited singlet states have been calculated following the TICT model [17–20]. During the evaluation of the potential energy surface, only the twisting angle θ_1 for donor group and θ_2 for acceptor group (Scheme 1) are varied, and the rest of the optimized geometrical parameters are frozen at the optimum parameters of the global minimum structure. The PECs for the first two excited singlet states are obtained using time dependent density functional theory (TDDFT) at the above level. The PECs with inclusion of solvent effect are also constructed using the above-mentioned basis set at DFT level. For the excited states, the TDDFT-PCM is used for the calculation of excited state surfaces. Though the TDDFT method of calculation fails to optimize the geometries for the excited states, results obtained using this method correlate well with the experimental data and are successfully used in several systems in recent times [12–15].

3. Results and discussion

3.1. Absorption spectra

As seen in Fig. 1, the absorption spectra of DMANAN in different solvents for identification of ground state species show a single broad band at ~360 nm in non-polar solvents (Table 1). This absorption band arises due to $\pi\pi^*$ transition of the naphthalene ring, and the band is red shifted compared to that of pure naphthalene

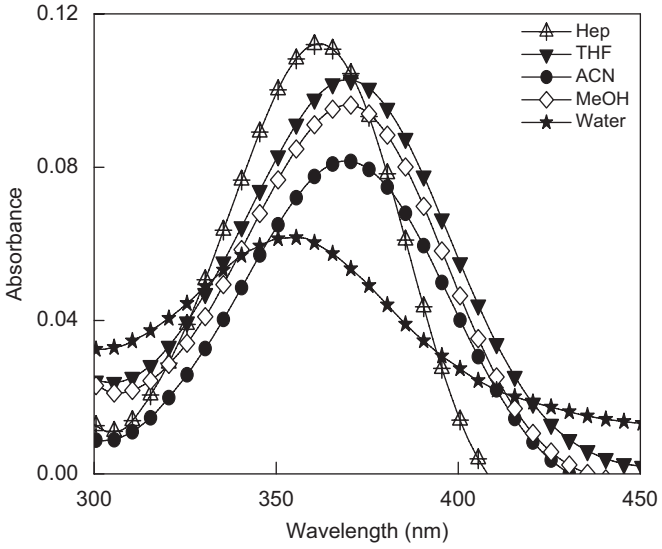

Fig. 1. Absorption spectra of DMANAN in different solvents at room temperature.

(λ_{abs} = ~275 nm) [36] due to the presence of the tertiary amino group and ethylene substitution at the ring aromatic chromophore. The same band shifts to the red side with increase of solvent polarity and is observed at ~375 nm in ACN solvent. An exception in this trend is observed in case of hydrogen-bonding solvent water, where the absorption maximum is found at ~355 nm and is much towards the blue side. Being a strong hydrogen-bonding solvent, water may form hydrogen-bonded solvated clusters which absorb at ~355 nm. Very similar observation was reported for several donor–acceptor systems [12–15]. The possible hydrogen-bonded clusters with polar protic solvents are shown in Scheme 2. The spectral characteristics are found to be similar to that of recently studied molecules MDMANA and EDMANA [33,34].

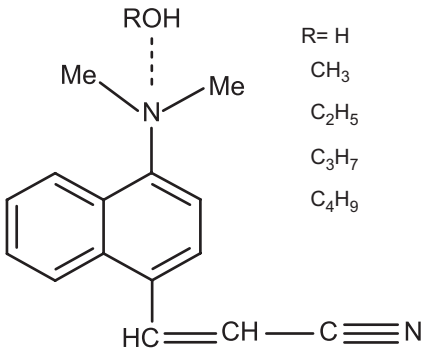

Scheme 2. Possible hydrogen-bonded clusters of DMANAN with protic solvents.

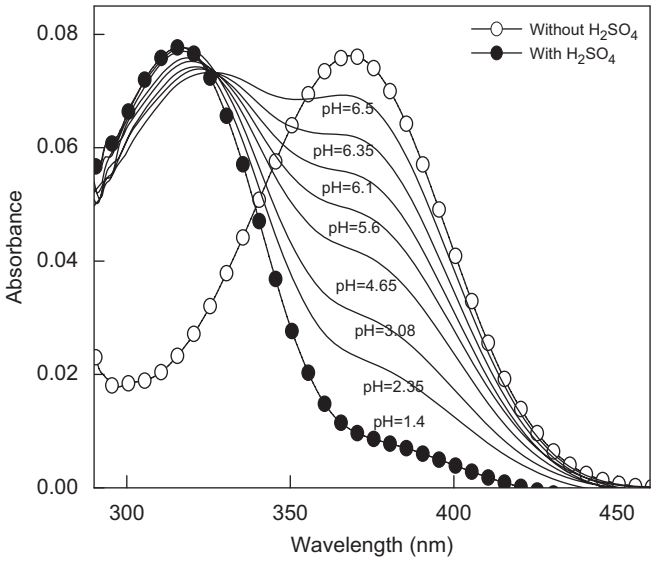

Fig. 2. Absorption spectra of DMANAN in the presence of acid at room temperature.

As shown in Fig. 2, addition of dilute H_2SO_4 to the methanolic solution of DMANAN results in the emergence of a higher energy absorption band at ~310 nm at the expense of ~370 nm band. As it was reported for several donor–acceptor CT molecular systems, the H^+ ion of acid can bind to the available lone pair of nitrogen atom of $-NMe_2$ group to form a protonated species (Scheme 3) which has less resonance stabilization compared to that of the neutral species and hence absorbs at the higher-energy side.

3.2. Emission spectra

Fig. 3a depicts the fluorescence emission spectra of DMANAN in solvents of varying polarity and the observed band maxima are given in Table 1. It can be seen in Fig. 3a that, in case of non-polar solvents, a single emission band at ~440 nm is observed upon excitation at ~360 nm, whereas for the same excitation dual fluorescence is observed in polar solvents. The higher energy band is observed at ~425 nm and the lower energy (LE) band

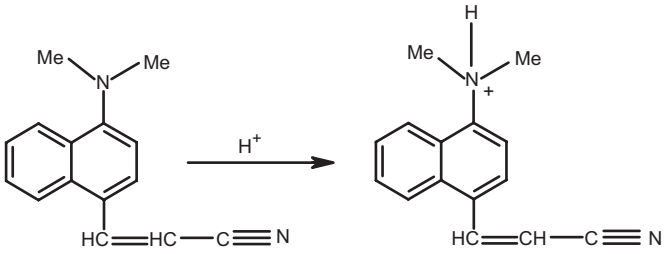

Scheme 3. Protonation process of DMANAN.

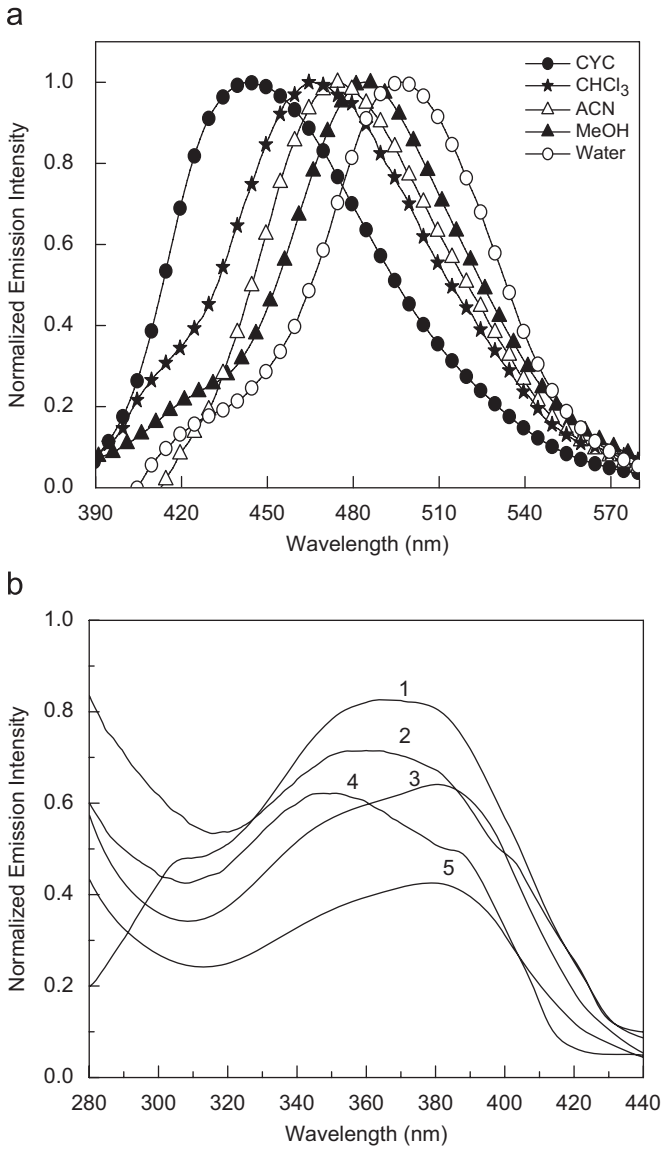

Fig. 3. (a) Emission spectra of DMANAN in different polarity solvents (λ_{ext} = 360 nm); (b) excitation spectra of DMANAN in different polarity solvents. 1— Hep (λ_{em} = ~443 nm), 2—ACN (λ_{em} = ~485 nm), 3—MeOH (λ_{em} = ~486 nm), 4—water (λ_{em} = ~498 nm) and 5—MeOH (λ_{em} = ~430 nm).

ranges between 473 nm in chloroform solvent and 498 nm in water. It is pertinent to mention here that naphthalene molecule shows its emission at ~320 nm [36]. With regard to donor–acceptor charge transfer systems of benzene type

[5,12–15] or similarly studied molecules, MDMANA and EDMANA [33,34], the higher energy emission band is assigned to emission from the LE state and the lower energy stronger emission from the CT state. This is also reflected in the fluorescence quantum yield values, where the fluorescence quantum yield values for the LE band are less than those for the CT band (Table 1). As seen in Fig. 3b, the excitation spectra of DMANAN for both the emission bands match perfectly well with the absorption spectra, thus indicating that both emission bands are originating from the same ground state species which absorbs at ~360 nm.

Quantitative analysis of the LE emission band indicates that the emitting species has a large dipole moment as the red shift of this emission band depends on the polarity of the solvent. This enhancement of the dipole moment in the excited state compared to the ground state leads to stabilization of the CT state with increasing solvent polarity. The solvent dipoles reorient themselves around the fluorophore to attain an energetically favourable arrangement and hence the red-shifted emission band shows its dependency on solvent polarity. As usual, the Fig. 4a shows the Lippert–Mataga plot of Stokes shift ($\Delta\nu$) vs. solvent parameter Δf (ε_r, n). According to Lippert–Mataga relation [37]

$$\nu_a - \nu_f = \frac{(\mu^* - \mu)^2}{2\pi\varepsilon_o hc\rho^3} \times f(\varepsilon_r \times n)$$

where $f(\varepsilon_r, n) = [(\varepsilon_r - 1)/(2\varepsilon_r + 1)] - [(n^2 - 1)/(2n^2 + 1)]$.

ν_a and ν_f correspond to the absorption and emission frequency, respectively, in a solvent with dielectric constant ε_r and n is the refractive index of the medium. The terms h, ε_0, c, ρ in the above equation are Planck's constant (6.6×10^{-34} J s), permittivity of vacuum (8.85×10^{-12} VC^{-1} m^{-1}), velocity of light (3×10^8 m s^{-1}) and Onsagar cavity radius, respectively. The terms μ and μ^* are dipole moments for the ground and excited state, respectively. The plot of $\Delta\nu$ vs. Δf shows linearity for non-polar and polar aprotic solvents. The value of ρ was calculated to be 5.06 Å at DFT level for the global minimum structure using B3LYP functional and 6–31G** basis set. From the ratio of the slope and $(\mu^* - \mu)^2/2\pi\varepsilon_o hc\rho^3$ of the Lippert–Mataga plot, the difference between excited state and ground state dipole moment is found to be 7.7 D. This large change in dipole moment from ground ($\mu = 6.98$ D) to the excited state ($\mu^* = 14.68$ D) occurs due to charge redistribution in the excited state by the process of CT from the electron-rich tertiary amino donor moiety to the acrylonitrile acceptor moiety.

However, in the case of protic solvents a deviation from linearity is found in the Lippert–Mataga plot. This indicates that the hydrogen-bonding solvent may have a different type of influence on the position of the red-shifted emission band [5,12–15]. As seen in Fig. 4b, it is found that position of the emission band (ν_f) in protic solvents varies linearly with the hydrogen-bonding parameter α [38]. This clearly supports the fact that the red-shifted band in protic solvents could have some emission component of the

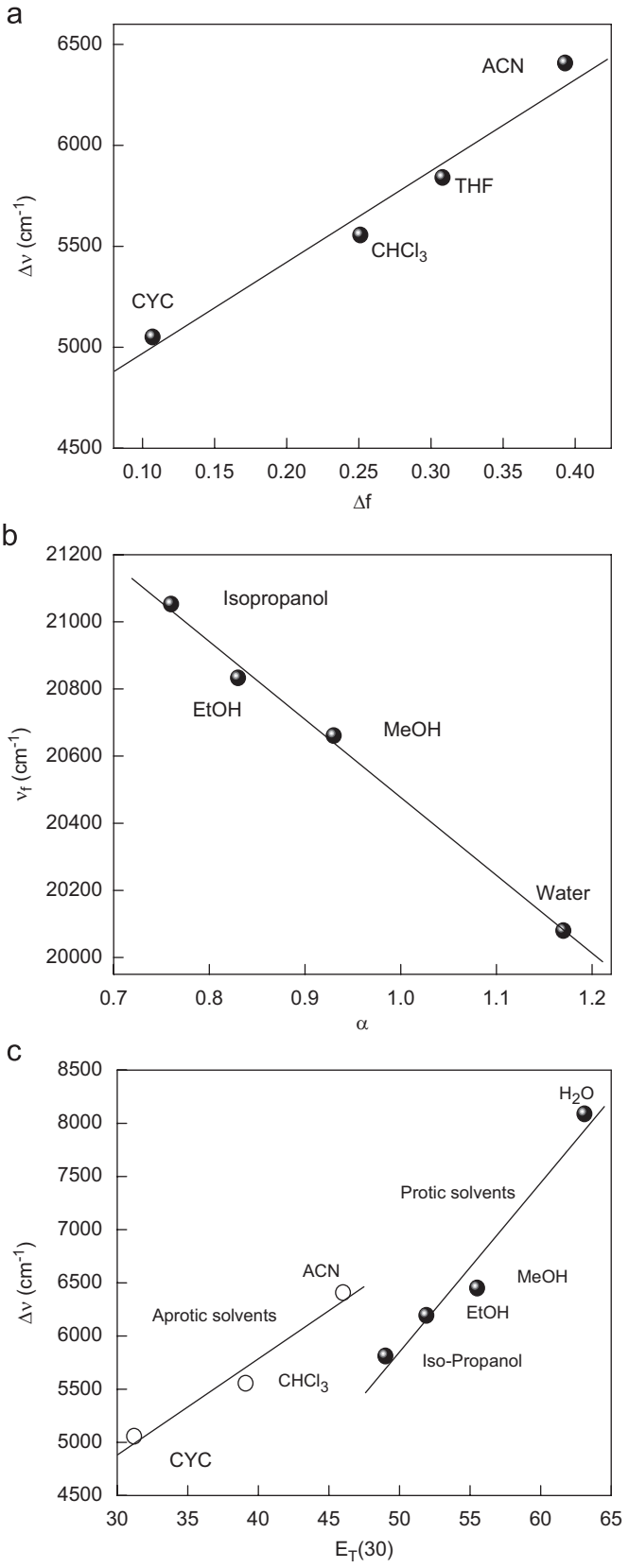

Fig. 4. Plot of (a) Stokes shift vs. solvent parameter (Δf) (Lippert plot), (b) fluorescence band maximum vs. hydrogen-bonding parameter (α) and (c) Stokes shift vs. $E_T(30)$ parameter of DMANAN.

hydrogen-bonded clusters, which ultimately shows red-shifted CT emission. As seen in Fig. 4c, the plot of Stokes shift vs. solvent polarity parameter $E_T(30)$ indicates that there are two types of interactions present in the system. Two set of straight lines in Fig. 4c—one for aprotic solvents and another for protic solvents—indicate that both the hydrogen-bonding and dipolar interactions are present for this system. To further reinforce the role of hydrogen bonding in the TICT process, we have performed an experiment to show the effect of temperature on the intensity of the CT band (Figs. 5a and b). As seen in Fig. 5a, the intensity of both the emission bands of DMANAN in MeOH solution decreases with increase of temperature, whereas the intensity of the CT band in acetonitrile (ACN) decreases but LE band does not show appreciable decrease in intensity with increase of temperature (Fig. 5b). In case of ACN solution, since there is no hydrogen-bonded complexation, decrease in CT emission intensity can be assigned to an increase in non-radiative decay process with increase of temperature. On the other hand, in the case of MeOH solution, decrease of intensity of red-shifted bands may be due to breaking of the intermolecular hydrogen bonding of the solvated complex (Scheme 2). Cazeau-Dubroca et al. [39] proposed that the tetragonal arrangement of amine side due to formation of H-bond with protic solvents in the ground state favours the TICT process. As seen in Table 1, the fluorescence quantum yield values in protic solvents are low compared to that of non-protic solvents. This observation also supports the fact that H-bonding plays a crucial role in non-radiative processes.

The emission spectra of methanolic solution of DMANAN in the presence of dilute H_2SO_4 are shown in Fig. 6. Addition of acid results in the increase in intensity of the LE emission band with a concomitant decrease in intensity of the CT band, with a clear isoemissive point at ~458 nm. In fact, the H^+ ion of acid binds to the lone pair of nitrogen atom of the dimethylamino group ($-NMe_2$), hindering the formation of the CT state or hydrogen-bonded complex, thereby decreasing emission from the red-shifted band. The protonated species emits its own local emission at the high-energy side (423 nm). However, the presence of CT emission, though much less prominent compared to the LE emission of the protonated species, may be due to the possibility of excited state deprotonation process. The protonated species deprotonates in the excited state potential energy surface to form the LE state of the neutral species, which then undergoes a transformation to the CT state, thus leading to CT emission.

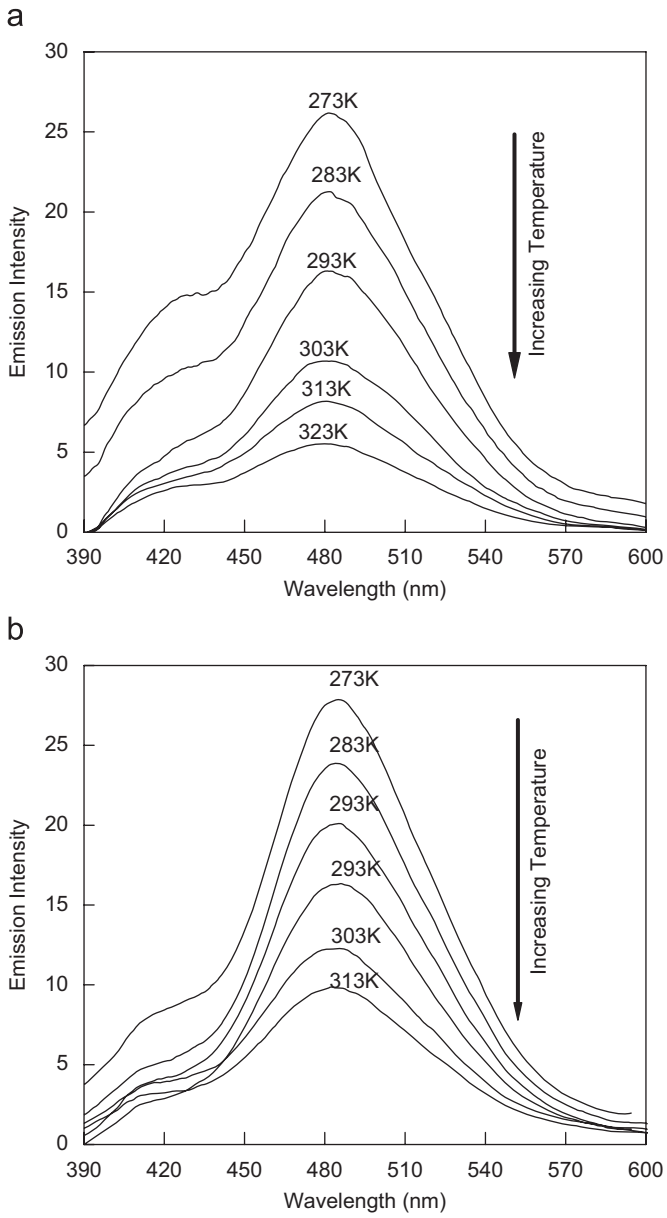

Fig. 5. Emission spectra ($\lambda_{ext} = 360$ nm) of DMANAN at different temperatures in (a) MeOH and (b) ACN solvent (arrow indicates increase of temperature).

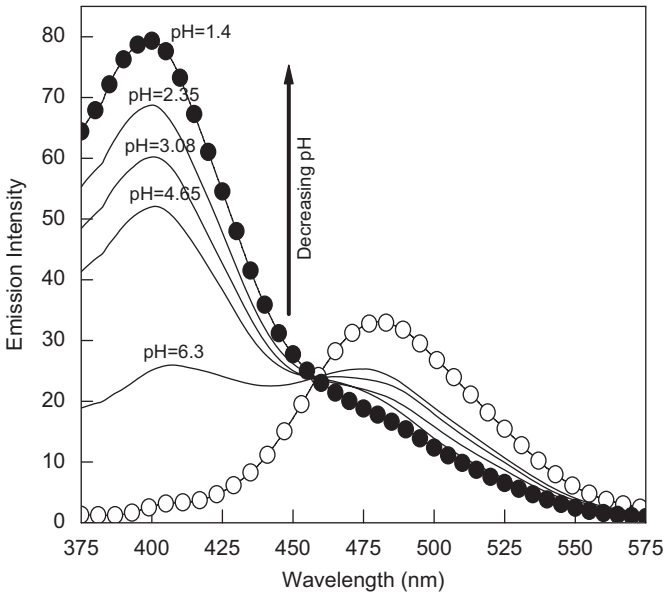

Fig. 6. Emission spectra ($\lambda_{ext} = 360$ nm) of DMANAN in the presence of acid (arrow indicates increase of acid concentration).

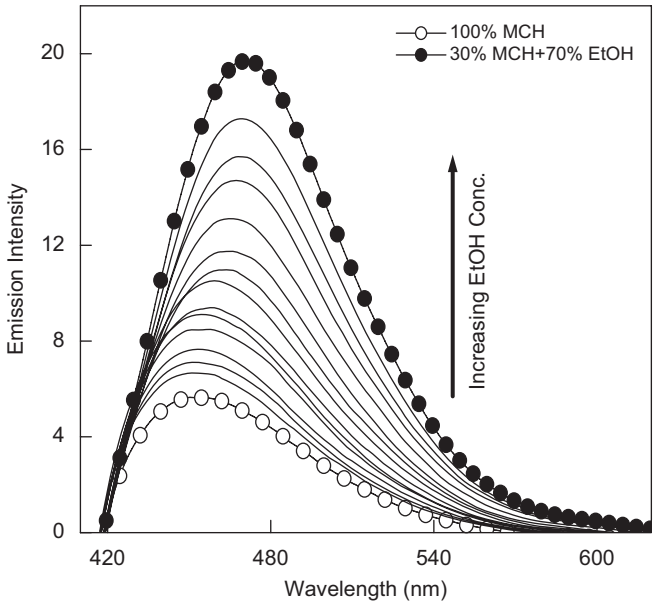

Fig. 7. Emission spectra ($\lambda_{ext} = 360$ nm) of DMANAN in methylcyclohexane + ethanol mixed solvent.

Fig. 7 shows the emission spectra of DMANAN in mixed solvent (MCH + EtOH). Addition of EtOH in MCH solution of DMANAN shows a red shift from ~440 to ~470 nm with increasing intensity of the red-shifted emission band. This observation indicates that the red-shifted emission band originates from the LE state upon relaxation and the shifted band in protic solvents originated from the hydrogen-bonded clusters.

4. Computational details

In order to correlate our experimental findings, we have performed theoretical calculations at DFT level using B3LYP functional and 6–31G** basis set, and the optimized parameters of the global minimum structure of DMANAN are given in Table 2. In the calculated minimum structure of DMANAN, the donor $-NMe_2$ group is found to be out of plane ($\theta_1 = 22^\circ$) of the naphthalene ring and the N-atom of the $-NMe_2$ group is pyramidal in its global minimum state in vacuo. As per the TICT model, such a pretwisted structure at the nitrogen center may favour the excited state CT process (17–20). Similar to that of the donor side, the π-orbitals of acceptor group are slightly titled with respect to the π-orbitals of the aromatic ring ($\theta_2 = 27.8^\circ$). Basically, two substituted groups (donor and acceptor) feel steric repulsion, named as 'peri hydrogen' interaction, with the C_5 and C_8 carbon atoms of the naphthalene ring and hence lie out of the plane of the aromatic ring. The potential energy surfaces along the donor and acceptor twist coordinates are shown in Figs. 8 and 9, respectively. As shown in Fig. 8a, further twisting of the donor angle leads to an increase in energy, with a maximum at $\theta_1 = 72^\circ$ for the S_0 state in vacuo. Then

Table 2
Optimized parameters of ground state geometry of DMANAN at DFT level with B3LYP functional and 6–31G** basis set (refer Scheme 1)

Bond lengths	Value (Å)	Angles	Value (°)
C_{10}–N_9	1.4679	$\angle C_{10}$–N_9–C_{11}	111.477
C_{11}–N_9	1.4563	$\angle C_{10}$–N_9–C_1	115.9132
N_9–C_1	1.4135	$\angle C_{11}$–N_9–C_1	116.975
C_1–C_2	1.3872	$\angle C_4$–C_{12}–C_{13}	125.700
C_2–C_3	1.4040	$\angle C_{13}$–C_{14}–N_{15}	178.966
C_3–C_4	1.3876	$\angle C_{11}$–N_9–C_1–C_2	22.230
C_4–C_{12}	1.4608	$\angle C_3$–C_4–C_{12}–C_{13}	−27.809
C_{12}–C_{13}	1.3524		
C_{13}–C_{14}	1.4238		
C_{14}–N_{15}	1.1653		

a decrease upto $\theta_1 = 92^\circ$ followed by an increase in energy is observed. This observation can be well accounted for if the 'peri effect' between the donor group and H-atom at the 8 position of the naphthalene ring is taken into consideration (Scheme 1). During the course of its twisting, the donor group feels steric interaction with this peri H-atom and the conformer becomes unstable. This also accounts for the initial twisting of the $-NMe_2$ group out of plane in the global minimum state and formation of two minima on the potential energy surface. Such an interaction is absent in benzene systems and hence the donor group may favour planar geometry in its global minimum state for benzene systems. Therefore, for DMANAN, the ground state shows an asymmetric double-well type of potential with a local and a global minimum. However, the energy difference between two conformers is high and it is likely that only the global minimum structure can exist in the ground state. As can be seen in Fig. 8a, the energy of the first excited state (S_1) also shows an asymmetric double-well potential, with a second minimum at $\theta_1 = 72^\circ$. The nature of the S_1 state surface is such that the molecule easily transforms from locally excited state to lowest energy twisted geometry through a small barrier. The second excited state (S_2) also shows a similar minimum at $\theta_1 = 72^\circ$. Since excitation to the second excited state requires far more energy than that of the first excited state, it is expected that the phenomenon of ICT occurs in the S_1 state. Calculation predicts a transfer of the initially excited species to the twisted CT state in the S_1 surface through a small barrier (0.98 kcal mol^{-1}). The evaluation of PECs has also been carried out in ACN solvent using the TDDFT-PCM model (Fig. 8b). The nature of the PECs for both the ground and the excited states is basically the same as obtained in vacuo. The twisted conformer in the S_1 state, however, becomes more stable in the presence of solvent and the barrier for the conversion from LE to CT state is lower (0.44 kcal mol^{-1}) compared to that of gas phase results (0.98 kcal mol^{-1}). The variation of oscillator strength and vertical excitation energy for the S_1 state is shown in Fig. 8c and Table 3. As shown in Fig. 8c, along the donor twisting path a red-shifted emission is expected

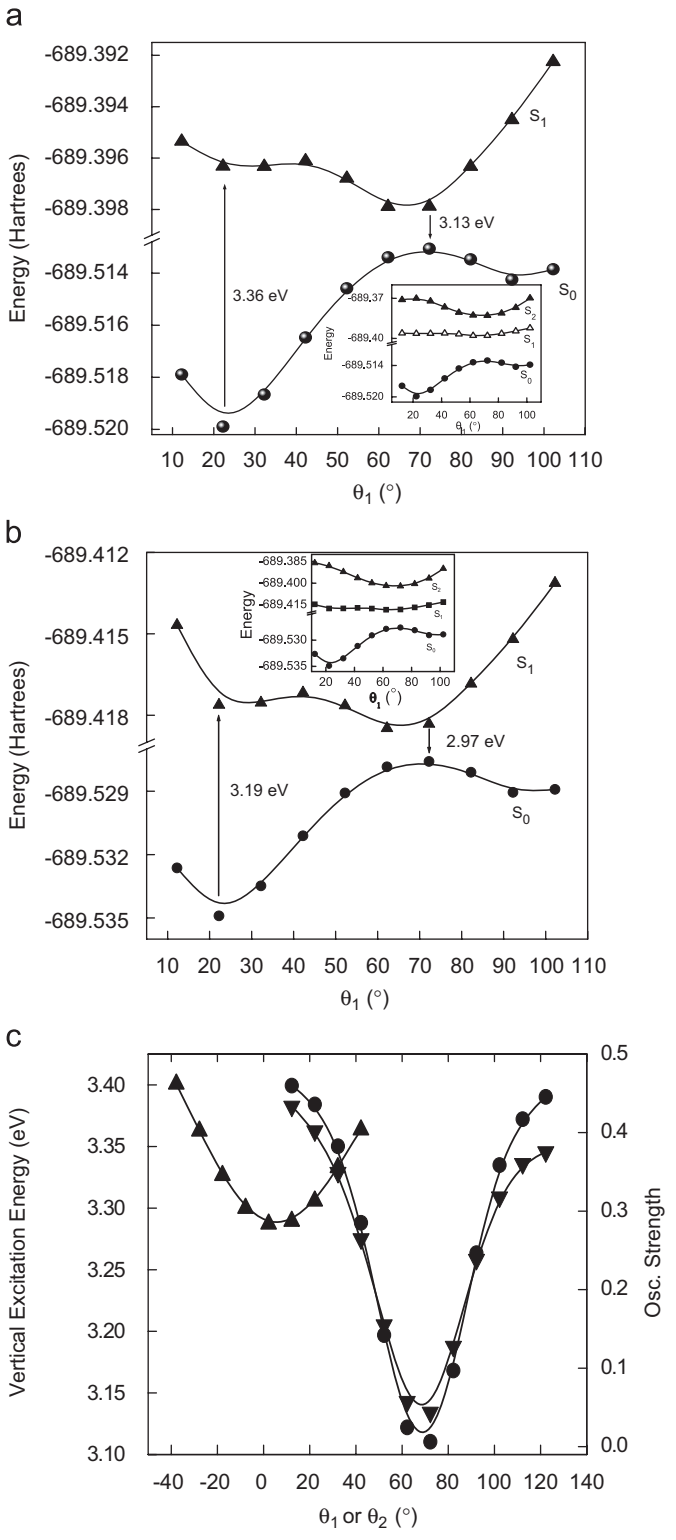

Fig. 8. Potential energy surfaces of DMANAN along the twisting of donor side (θ_1) in (a) vacuum and (b) in ACN solvent (DFT/6-31G**/B3LYP). Inset: PECs for the ground and first two low-energy excited states; (c) plot of vertical excitation energy (-▼- for donor and -▲- for acceptor twisting) and oscillator strength (-●-) for donor twisting vs. respective twist angles θ_1 and θ_2.

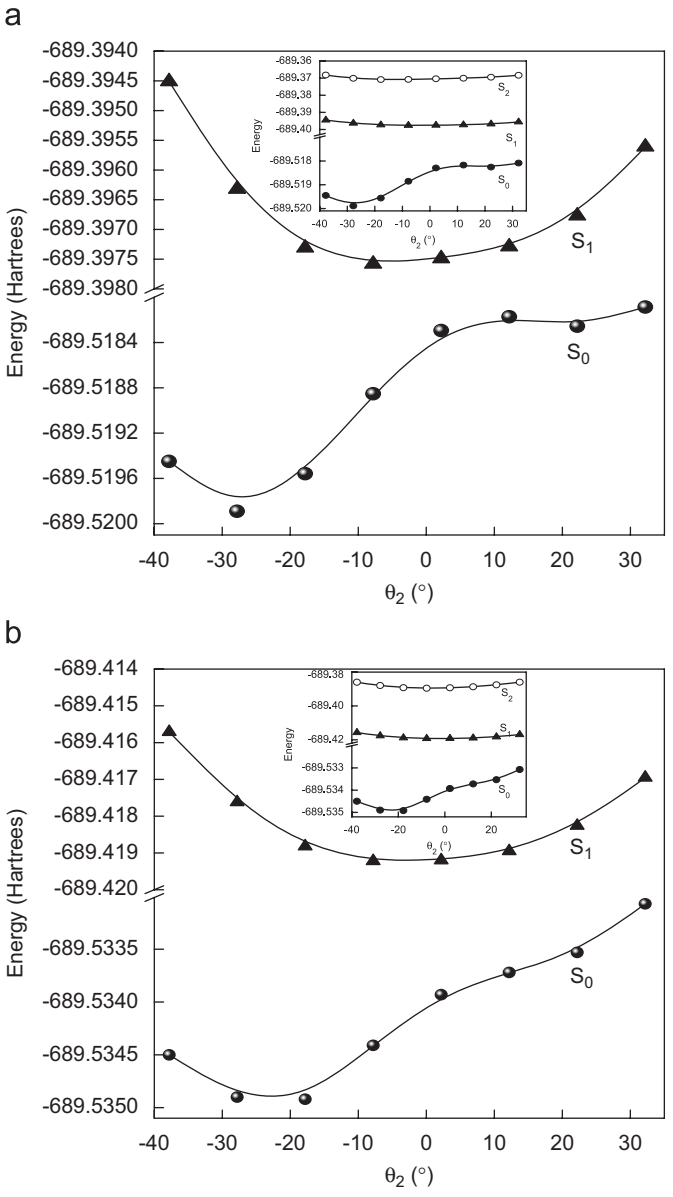

Fig. 9. Potential energy surfaces of DMANAN along the twisting of acceptor side (θ_2) in (a) vacuum and (b) in ACN solvent (DFT/6-31G**/B3LYP). Inset: PECs for the ground and first two low-energy excited states.

theoretically and the red shift in ACN solution is high and correlates well with the experimental emission band. Although the acceptor-twisting path also provides a red-shifted emission, the agreement of theoretical emission energy with the experimental values are very poor. As seen in Figs. 9a and b, the twisting of the acceptor group (θ_2) produces a single well on the S_0 surface and a single minimum flat-type potential in the S_1 surface both in vacuum and in ACN solvent. S_0 twisting at the acceptor site theoretically does not predict any LE emission in non-polar solvents. Instead, it predicts only a broad red-shifted band both in vacuum and ACN solvent, which is contrary to the experimental observation. As seen in Table 3, the experimental and theoretical values for absorption and

Table 3
Computed parameters of DMANAN in vacuum and acetonitrile solvents using DFT method with B3LYP hybrid functional and 6–31G** basis set

Medium	States	Absorption (eV)		Emission (eV)		
		E_{exp}	E_{th}	$E_{th.}$[a]	$E_{th.}$[b]	E_{exp}
Vacuo	S1	3.45	3.36 (0.4359)	3.13 (0.0063)	3.29 (0.4397)	2.82[c]
	S2	–	4.08 (0.0042)	3.54 (0.3266)	4.03 (0.0046)	–
ACN	S1	3.35	3.19 (0.5395)	2.97 (0.0077)	3.12 (0.5619)	2.56
	S2	–	3.99 (0.0269)	3.42 (0.4046)	3.94 (0.0051)	–

Values in parentheses are calculated oscillator strength.
E_{th} is the calculated energy value ($E_{excited}$–E_{ground}) at DFT level (B3LYP/6-31G(d,p)).
E_{ex} is the experimental value.
[a]Emission energy due to twisting of –NMe_2 group.
[b]Emission energy due to twisting of –CH═CH–CN group.
[c]The experimental value in n-hexane solvent.

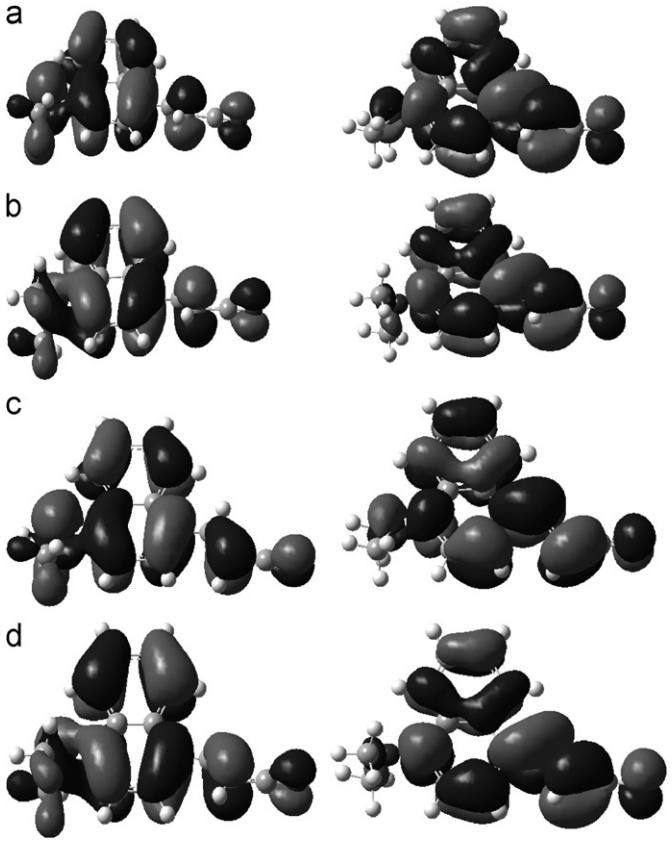

Fig. 10. Molecular orbital pictures (HOMO and LUMO) of DMANAN for the (a) normal, (b) donor twisted, (c) acceptor twisted geometry in vacuo and (d) donor twisted geometry in ACN solvent.

emission energies for vacuo and in ACN solvent (for donor group twisting) match reasonably well and hence our prediction is supportive to experimental results.

The HOMO–LUMO molecular orbital pictures for the global minimum structure and for different twisting geometries are shown in Fig. 10. For the global minimum state, the nitrogen lone pair is found to be more or less uniformly distributed over the entire π system of the naphthalene ring for both HOMO (π) as well as LUMO (π^*). Hence, the transition is of π–π^* type, which is allowed with high oscillator strength (0.4359). In the donor twisted state, the electron density is mainly over the N-atom and the HOMO (n) is basically a non-bonding orbital. In the LUMO (π^*) orbital the electron density is located over acceptor group side. Thus the transition is the forbidden n–π^* type. This is also revealed from the oscillator strength values, which decrease from 0.4359 in the global minimum state to 0.0063 in the twisted state. In this twisted geometry the lone pair of nitrogen is localized at the nitrogen centre and is available for transfer to the acceptor group. The HOMO and LUMO orbital pictures in the case of acceptor twisting are found to be similar to that of the global minimum state. At the donor twist geometry for both in vacuum and ACN solvent, the nitrogen lone pair is localized (HOMO orbital) compared to a delocalized HOMO orbital for the global minimum and acceptor twist state. The localized lone pair at the donor twisted geometry favours the CT process in the twisted decoupled state. Though n–π^* transition is symmetry forbidden, it is energetically generated through Frank-Condon excitation and the CT state is generated through a small barrier crossing on the S_1 surface.

5. Conclusion

In the present work, we have studied absorption and emission spectroscopy in combination with quantum chemical calculations of the title molecule DMANAN and established the existence of different ground and excited state species. The LE state relaxes to the twisted CT state, which gives a red-shifted emission, and this emission is sensitive to solvent polarity, pH of the medium and temperature. The formation of hydrogen-bonded clusters with protic solvents is established from the blue shift of the absorption band and linear dependence of emission band with hydrogen-bonding parameter. Structurally, the molecule shows a pretwisted geometry at the donor and acceptor site in the ground state. Theoretical PECs for the ground and first two singlet excited states at DFT level indicate that the donor twist coordinate supports ICT reaction over acceptor twist coordinate in the S_1 state. Theoretical PECs using TDDFT-PCM method predict well

the solvent polarity dependence of the red-shifted emission band. A decoupled donor–acceptor geometry with localized lone pair at the donor centre may be responsible for the formation of CT state and hence the solvent polarity dependence of red-shifted emission is observed in DMANAN molecule.

Acknowledgements

NG acknowledges DST, India (Project no.SR/S1/PC-1/2003) for financial support. RBS and SM are also grateful to CSIR, New Delhi for Senior Research Fellowship.

References

[1] E. Lippert, W. Luder, H. Boss, in: A. Mangini (Ed.), Advances in Molecular Spectroscopy, Pergamon Press, Oxford, 1962, p. 443.
[2] W. Rettig, B. Bliss, K. Dimberger, Chem. Phys. Lett. 305 (1999) 8.
[3] J. Herbich, J. Waluk, Chem. Phys. 188 (1994) 247.
[4] M. Maus, W. Rettig, D. Bonafoux, R. Lapouyade, J. Phys. Chem. A 103 (1999) 3388.
[5] P.R. Bangal, S. Panja, S. Chakravorti, J. Photochem. Photobiol. A: Chem. 139 (2001) 5.
[6] P. Hazra, D. Chakrabarthy, N. Sarkar, Langmuir 18 (2002) 7872.
[7] S. Sumalekshmy, K.R. Gopidas, J. Phys. Chem. B 108 (2004) 3705.
[8] V. Thiagarajan, C. Selvaraju, E.J. Padma Malar, P. Ramamurthy, Chem. Phys. Chem. 5 (2004) 1200.
[9] K.A. Zachariasse, S.I. Druzhinin, W. Bosch, R. Machinek, J. Am. Chem. Soc. 126 (2004) 1705.
[10] J.S. Yang, K.L. Liau, C.M. Wang, C.Y. Hwang, J. Am. Chem. Soc. 126 (2004) 12325.
[11] S. Murali, W. Rettig, J. Phys. Chem. A 110 (2006) 28.
[12] A. Chakraborty, S. Kar, N. Guchhait, J. Photochem. Photobiol. A: Chem. 181 (2006) 246.
[13] A. Chakraborty, S. Kar, N. Guchhait, Chem. Phys. 324 (2006) 733.
[14] A. Chakraborty, S. Kar, N. Guchhait, Chem. Phys. 320 (2006) 75.
[15] A. Chakraborty, S. Kar, N. Guchhait, J. Phys. Chem. A 110 (2006) 12089.
[16] Y.H. Kim, D.W. Cho, M. Yoon, D. Kim, J. Phys. Chem. 100 (1996) 15670.
[17] R. Hayashi, S. Tazuke, C.W. Frank, Macromolecules 20 (1987) 983.
[18] J.A. Bautista, R.E. Connors, B.B. Raju, R.G. Hiller, F.P. Sharples, D. Goszlota, M.R. Wasielewski, H.A. Frank, J. Phys. Chem. B 103 (1999) 8751.
[19] A. Kohn, C. Hattig, J. Am. Chem. Soc. 126 (2004) 7399.
[20] W. Rettig, B. Zietz, Chem. Phys. Lett. 317 (2000) 187.
[21] B. Mennucci, A. Toniolo, J. Tomasi, J. Am. Chem. Soc. 122 (2000) 10621.
[22] Z.R. Grabowski, K. Rotkiewicz, A.D. Siemiarezak, J.D. Cowley, W. Bauman, Nouv. J. Chin. 3 (1979) 443.
[23] K. Rotkiewicz, K.H. Grellmann, Z.R. Grabowski, Chem. Phys. Lett. 19 (1973) 315.
[24] Z.R. Grabowski, K. Rotkiewicz, A. Siemiarezak, J. Lumin. 18 (1979) 420.
[25] J. Catalan, C. Diaz, V. Lopez, P. Perez, R.M. Claramunt, J. Phys. Chem. 100 (1996) 18392.
[26] C. Rulliere, Z.R. Grabowski, J. Dobkowski, Chem. Phys. Lett. 137 (1987) 408.
[27] K.A. Zachariasse, Chem. Phys. Lett. 320 (2000) 8.
[28] A. Sobolewski, W. Domcke, Chem. Phys. Lett. 250 (1996) 428.
[29] K.A. Zachariasse, M. Grobys, T. von der Haar, A. Hebecker, Y.V. Iiichev, Y.B. Jiang, O. Morawski, W. Kuhnle, J. Photochem. Photobiol. A: Chemistry 102 (1996) 59.
[30] K.A. Zachariasse, M. Grobys, T. von der Haar, A. Hebecker, Y.V. Iiichev, Y.B. Jiang, O. Morawski, I. Ruckert, W. Kuhnle, J. Photochem. Photobiol. A: Chemistry 105 (1997) 373.
[31] E.M. Kosower, H. Kannety, J. Am. Chem. Soc. 105 (1983) 6236.
[32] E.M. Kosower, H. Kannety, H. Dodluk, G. Striker, T. Jovin, H. Boni, D. Huppert, J. Phys. Chem. 87 (1983) 2479.
[33] S. Mahanta, R.B. Singh, S. Kar, N. Guchhait, J. Photochem. PhotoBiol. A: Chem. 194 (2007) 318.
[34] R.B. Singh, S. Mahanta, S. Kar, N. Guchhait, Chem. Phys. 342 (2007) 33.
[35] M.J. Frisch et al., Gaussian 03, Revision B.03, Gaussian, Inc., Pittsburgh, PA, 2003.
[36] H. Du, R.A. Fah, J. Li, A. Corkar, J.S. Lindsay, J. Photochem. Photobiol. 68 (1998) 141.
[37] N. Mataga, H. Chosrowjan, S. Taniguchi, J. Photochem. Photobiol. C: Photochem. Rev. 6 (2005) 37.
[38] R.W. Taft, M.J. Kamlet, J. Am. Chem. Soc. 98 (1976) 2886.
[39] C. Cazeau-Dubroca, S. Ait Lyazidi, P. Cambou, A. Peirigua, P. Cazeau, M. Pesquer, J. Phys. Chem. 93 (1989) 2347.